SELF-CHANNELLING OF LASER PULSES AT RELATIVISTIC INTENSITIES IN PREIONIZED PLASMAS

M.Borghesi[1)], A.J.Mackinnon[1)], L.Barringer[1)], R.Gaillard[1)], L.Gizzi[2)], C.Meyer[1)], O.Willi[1)], A.Pukhov[3)], J.Meyer-ter-Vehn[3)]

1) The Blackett Laboratory, Imperial College of Science Technology and Medicine, London
2) Istituto di Fisica Atomica e Molecolare - CNR (Pisa), Italy
3) Max-Planck-Institut für Quantenoptik, Garching (Germany)

INTRODUCTION

The study of the interaction of intense laser pulses with plasmas is relevant for applications such as particle acceleration by plasma waves[1)] and the fast ignitor scheme[2)] for Inertial Confinement Fusion. These applications require the pulse to propagate over several Rayleigh lengths without considerable energy loss. For sufficiently powerful, spatially uniform laser pulses, self-guiding of the pulse can be achieved due to relativistic effects[3)]. Indeed, channelled propagation at relativistic intensities through initially neutral gases has been already observed in various experiments[4)], while observations of relativistic channelling in pre-ionised plasmas of near critical density, particularly relevant for fast ignitor applications, have been reported only recently[5)]. In particular, for laser pulses far above the threshold for relativistic filamentation, three-dimensional particle-in-cell (3D PIC)[6)] predicted the formation of a narrow, single propagation channel. The simulations revealed the importance of relativistic electrons travelling with the light pulse and generating multi-megagauss magnetic fields that pinch the electrons.

Here we report about a series of experiments performed at the Rutherford Appleton Laboratory to study the relativistic channelling of ultra-intense picoseconds pulses in pre-ionised plasmas[7)]. Some of the data here discussed have been already presented in last year's RAL annual report[8)].

EXPERIMENTAL SET-UP

The experiment was performed using the Vulcan Nd:glass laser in the chirped pulse amplification (CPA) mode. The targets were plastic (CH or Formvar) films with a thickness between 100 and 500 nm. The plasma was preformed by a 400 ps pulse, frequency doubled in a KDP crystal to λ=0.527 μm, which was focused onto target, in a spot between 200 and 300 μm in diameter, at an irradiance below 10^{13} W/cm^2. A 1.054 μm CPA interaction pulse of 1-3 ps in duration was focused into the preformed plasma. Both the heating and the interaction pulse were focused onto target by the same F/4.5 off-axis parabola (OAP). The green heating beam was injected into the short pulse beamline through the back of the last turning mirror before the OAP. A small divergence was imposed on the heating beam before the interaction chamber by a telescope in order to obtain a larger focal spot. The beam was focused in a 12 - 15 μm full width at half maximum (FWHM) focal spot. With an average interaction power of 10 TW, an incident irradiance between 3 and 9x10^{18} W/cm^2 was obtained. The delay between heating and interaction pulses was varied, allowing interaction with the plasma at different stages of its evolution. The plasma was diagnosed with a temporally independent probe pulse which was split-off from the uncompressed interaction beam. The probe beam was compressed by a pair of gratings and frequency doubled in a KDP crystal resulting in a probe wavelength of 0.527 μm and a pulse duration of a few picoseconds. The spatial resolution determined by the optical system was around 2 - 3 μm. Time resolved density maps of the plasma (limited to densities lower than 10^{20}/cm^3 due to refraction) were obtained with a Nomarski modified interferometer. The optical emission from the plasma was also imaged, in a direction transverse to the propagation axis. The magnetic fields generated in the plasma during the interaction were measured using a time-resolved polarimetric technique. For these measurements, particularly sensible to emission noise, the probe wavelength was Raman-shifted to λ=620 nm. Also, spectra of the backscattered radiation were collected with an optical grating spectrometer, using a 1200 lines/mm grating (linear dispersion 15 Å/mm).

EXPERIMENTAL RESULTS AND SIMULATIONS

Self-channelling of the CPA pulse appeared to be a typical feature of the interaction in the investigated experimental conditions and was detected via optical probe measurements. In fig.1 the spatially resolved second harmonic radiation emitted during the interaction of a 10 TW pulse with the preformed plasma is shown. The measured density profile is also presented (1-D simulations predict that the plasma is fully ionised, with a peak density of about 5x10^{20}/cm^3). The channel-like emission is time-integrated and is due to second harmonic (2ω) light emitted during the interaction, produced via non-linear processes in correspondence with the large density and intensity gradients present inside the channel. It can therefore be interpreted as a signature of the spatial extent of the interaction beam in the plasma. The average diameter of the channel is about 5 μm and its length about 130 μm. The channel changes in size periodically over distances of 15 - 20 μm with the transverse dimension varying within a few microns. From comparison with the preformed plasma profile, it can be seen that the laser pulse focuses down to 5 μm in size at a density of around 0.05 times the critical density n_c (n_c~1x10^{21}cm^{-3} for λ=1 μm). It should also be noted that the laser power was about 25 times the threshold power for relativistic self-focusing, $P_{th}=17\omega^2/\omega_p^2 \approx 0.4$ TW at this density.

Evidence of channelling was also obtained from interferometric measurements. The interferogram of fig.2 was taken at about 5 ps after the interaction (the preformed plasma density profile is also shown). A front (due to the shock wave expanding in the preformed plasma) produced by the short pulse while focusing down into the channel is clearly visible.

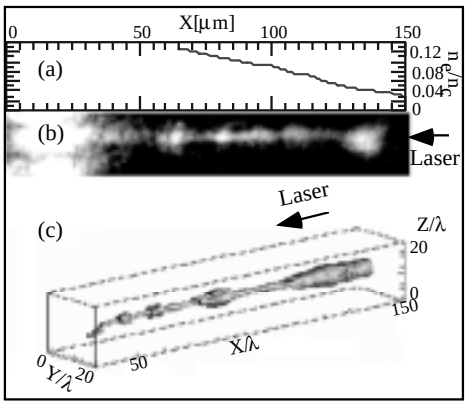

Fig.1. Channelling of a ps, 1.054 mm, 10 TW pulse during propagation through a preformed plasma: (a) preformed plasma density; (b) second harmonic emission channel; (c) 3-D PIC simulation: a perspective snapshot of the self-focusing pulse after 150 laser cycles (i.e. about 0.5 ps); the plotted surface corresponds to 67% of the cycle-averaged maximum intensity $<I_{max}>$. X is the distance from the original target position.

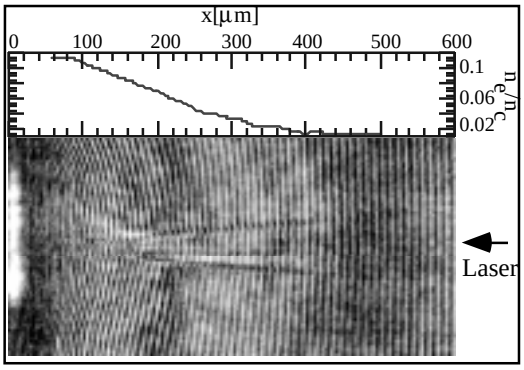

Fig.2. Interferogram taken 5 ps after the interaction of a 1.5 ps, 10 TW pulse with a preformed plasma. The density profile of the preformed plasma is also shown.

The laser pulse appears to be focused with an F/4.5 cone up to a background density of approximately 0.07 n_C at a distance of about 200 mm from the original target position. Beyond that density, it self-focuses into the channel. The experiment has been simulated with the 3D PIC code VLPL (Virtual Laser Plasma Laboratory), recently developed at the Max Planck Institute (Garching) for massive parallel processing (MPP). The simulation results are presented in figs. 1(c) and 3. The intensity distribution $<I>$ is shown in fig.1(c) for a time close to the peak of the pulse. After an initial unstable phase, the incident beam self-focuses into a narrow single channel at a density of about 0.07 n_C, according to the process described in ref.6. The channel width pulsates as the pulse defocuses and refocuses with a characteristic period of 15 -30 l. The maximum intensity $<I_{max}>$ varies accordingly with peaks up to 10 I_0. These results closely reproduce the experimental observations. The channel of fig.1(c) is further analysed in fig.3 by plotting the electron density for a Y,Z cross-section at $X = 80\ l$ and also as a line profile, normalised to the critical density n_C. One observes that electrons are expelled from the channel region and form a radially outgoing shock. An important feature governing the channel dynamics are currents of relativistic electrons travelling with the light beam and generating quasi-stationary magnetic fields[6]. The relativistic electrons modify the index of refraction n_r in the neighbourhood of the channel.

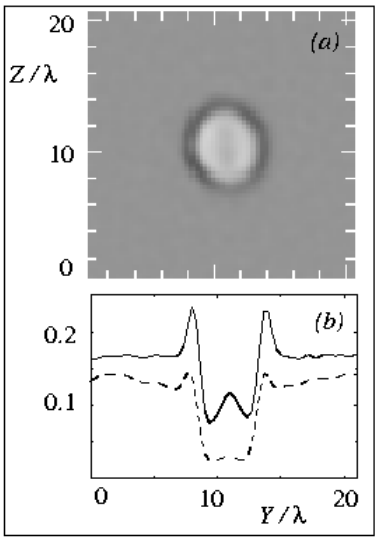

Fig.3. 3-D PIC simulation: electron density in units of the critical density n_C for Y,Z plane at $X=80\lambda$, after 150 laser cycles: a) 2D plot using linear grey scale; b) cut through centre in Y direction: n_e/n_C (solid line), $n_e<\gamma^{-1}>/n_C$ (dashed line).

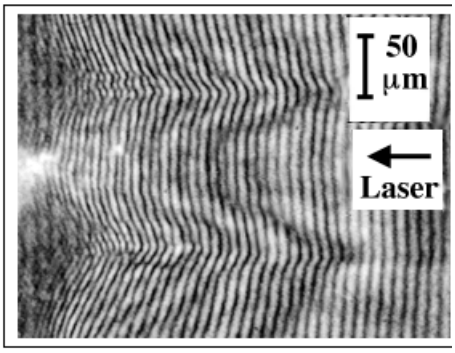

Fig.4. Interferogram recorded 65 ps after the interactic

This can be seen in fig.3, where the quantity $n_e<\gamma^{-1}>/n_C = 1 - n_r^2$ is plotted as a dashed line (the factor $<\gamma^{-1}>$, locally averaged, accounts for the mass increase). A "relativistic valley" has formed, about 20 λ wide. At its centre, a deeper density depression is produced by both electron expulsion and relativistic effects, and most of the light is guided into it.

The main feature observed in the 2ω backscattered spectra was a red-shifted broadening typically up to 40-50 nm. The broadening of the 2ω spectra can be explained as a Self Phase Modulation effect in the context of the channelling assumption discussed above. During the channel formation, the pulse travels through a medium in which the refractive index is rapidly varying. As a consequence, its phase is modulated. Since the derivative of the refractive index stays positive during the pulse propagation, the broadening is on the red side of the spectrum. The order of magnitude of the broadening expected, $\Delta\lambda/\lambda$, can be estimated supposing that the pulse propagates, during the channel formation, in an initially uniform plasma : $\Delta\lambda/\lambda \approx L\Delta n_r/(c\tau)$, where L is the length of the channel, Δn_r the maximum variation of refractive index, c the speed of light, τ the cavitation time. Using parameters close to the experimental ones, such as L=130 μm, τ=0.5 ps, Δn_r=0.07 (as in fig.3(b)) and λ=0.5 μm, one obtains Δλ≈30 nm, which is of the same order of magnitude of the measured broadenings.

After the pulse has traversed the plasma, the channel boundaries quickly expands. In fig.4 an interferogram of the channel after 65 ps is shown, when it has expanded to a radius of about 60 μm. At this time the density inside the channel is still about 40% of the background density. The temporal evolution of the channel size is shown in fig.5.

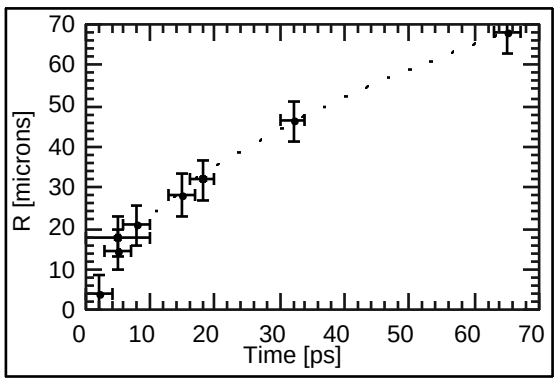

Fig.5. Temporal evolution of the channel radius (solid circles). The dashed line represents the best fit using a function proportional to $t^{1/2}$, while the empty squares represent the spatial extent of the inner Faraday rotation patterns in the polarigrams in fig.6.

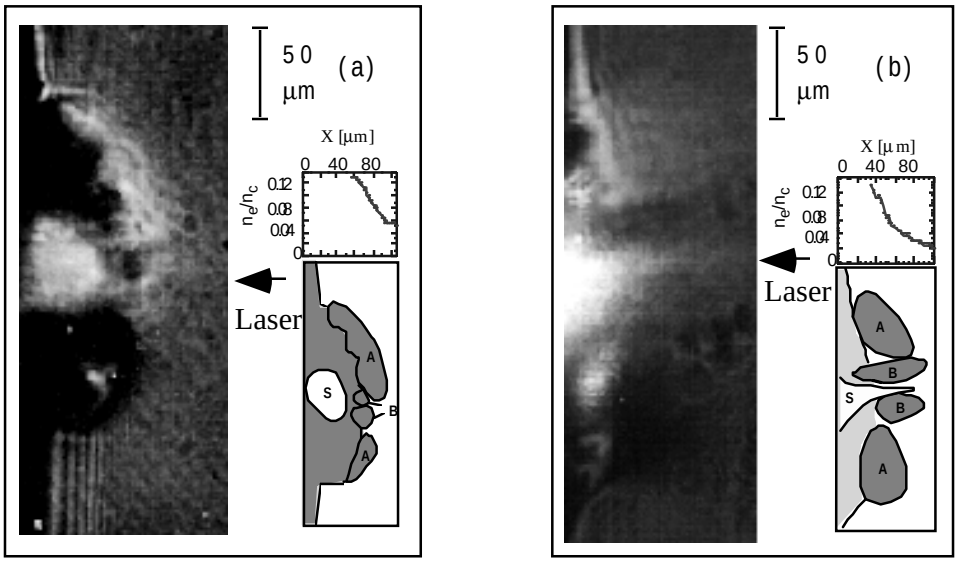

Fig.6. Polarigrams taken: (a) during the interaction of a 3 ps , 8 TW pulse, with the preformed plasma (probe duration Å 5 ps, with a maximum timing error of 8-10 ps); (b) 18 ps after the interaction of a 1.5 ps, 10 TW pulse with the preformed plasma (probe duration 2 ps , timing precision comparable with the probe pulse duration). The preformed plasma density profiles are also shown in the figure. In the sketches the outer dark-bright pattern are indicated with "A", the inner dark-bright pattern with "B" and the self-emission with "S".

The channel boundaries move out with an initial speed of about 5 10^8 cm/s, and expand with time following a $t^{1/2}$ dependence, as predicted from shock waves theory.

An important issue also investigated during the experiment was the generation of magnetic fields in the plasma as a consequence of the interaction (see also ref.9). The polarigrams shown in fig.6 were taken respectively during and 18 ps after the interaction, in two separate experiments. The Faraday rotation patterns detected show that two different types of toroidal fields are generated in the plasma as a consequence of the interaction. A "dark-bright " pattern (brighter than the background above the laser axis, darker below) is visible in the outer region of the plasma, as indicated in the figure. Another similar rotation pattern, but reverted with respect to the outer one, is visible close to the laser axis. While the outer rotation corresponds to a B-field directed as conventional thermoelectric field, the inner pattern corresponds to a toroidal field of opposite direction, with an amplitude that can be estimated to be in the range 1-10 MG [9], and consistent with the generation mechanism described in ref.6-7, i.e. with a current of fast electrons travelling on axis together with the laser pulse, and spatially separated return currents. During the expansion this field appears to stay confined within the expanding channel walls and affects the plasma behaviour, as it has been observed experimentally. In the interferogram of fig.7, taken 5 ps after the interaction, a density spike on axis, at the centre of the expanding channel suggested (as also observed in combined PIC + Magneto-hydrodynamic simulations[9]) that, within the shot-to-shot variability of the plasma conditions, the magnetic pressure may dominate over the thermal pressure in the region where the B-field peaks, and pinch the plasma on axis.

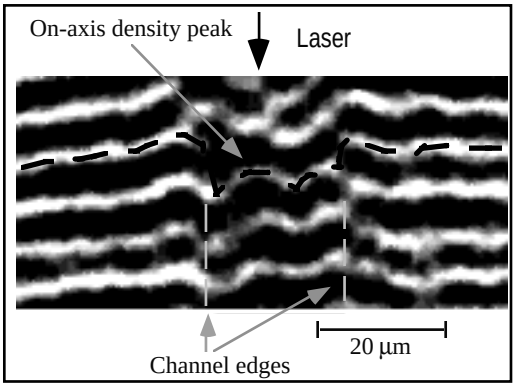

Fig.7 Interferogram taken 5 ps after the interaction. A fringe shift at the centre of the channel, corresponding to a density spike, is clearly visible.

CONCLUSION

The results of a series of experiment performed using the CPA Vulcan pulses indicate that the propagation of pulses at relativistic intensity through pre-ionised plasmas is characterised by relativistic self-channelling. This phenomenon was detected using optical probing diagnostics, and modelled using 3-D PIC simulations, that closely reproduced the experimental results and contributed to the understanding of the complex interaction scenario.

REFERENCES

1) E.Esarey *et al.*
IEEE Trans. Plasma Sci. 24, 252 (1996)

2) M. Tabak *et al.*
Phys. Plasmas 1, 1621 (1994)

3) P. Sprangle and E. Esarey
Phys. Fluids B 4, 2241 (1992)

4) A.B.Borisov *et al*
Phys. Rev. Lett. 68, 2309 (1992); P.Monot *et al.*, Phys. Rev. Lett. 74, 2953 (1995)

5) P.E.Young and P.R.Bolton
Phys. Rev. Lett., 77, 4556 (1996)

6) A. Pukhov and J. Meyer ter Veh
Phys. Rev. Lett. 76, 3975 (1996)

7) M.Borghesi *et al*
Phys. Rev. Lett. 78, 879 (1997)

8) M.Borghesi *et al*
Rutherford Appleton Laboratory Annual Report 1995-1996, RAL-TR-96-076, p.16 (1997)

9) M.Borghesi *et a*
in preparation (1997)